

# AN INTEGRATED SENSOR ORIENTATION SYSTEM FOR AIRBORNE PHOTOGRAMMETRIC APPLICATIONS

M. J. Smith <sup>a,\*</sup>, N. Kokkas <sup>a</sup>, D.W.G. Park <sup>b</sup>

<sup>a</sup> Faculty of Engineering, The University of Nottingham, Innovation Park, Triumph Road, Nottingham NG7 2TU, UK  
(martin.smith, nikolaos.kokkas)@nottingham.ac.uk

<sup>b</sup> Geospatial Research Centre (NZ) Ltd, Christchurch, New Zealand (now at <sup>a</sup>)  
david.park@nottingham.ac.uk

## Commission 1

**KEY WORDS:** Georeferencing, integrated systems, geometric, imagery, calibration, block, digital, cost-effective

### ABSTRACT:

There are now available excellent integrated sensor orientation systems for the direct measurement of sensor position and attitude using GPS and IMU technology. With the maturity of these systems has come a wider interest in using this technology in an ever-increasing range of applications. With a variety of applications, there becomes a need for a variety of solutions, balancing quality and cost. The Geospatial Research Centre (NZ) Ltd (GRC) has been developing integrated sensor orientation technology and exploring the applications for low cost but effective solutions. A range of sensors has been considered including thermal cameras and digital single lens reflex cameras. At the present time there is a rapid pace of development in digital single lens reflex cameras which is providing them with added photogrammetric potential.

The result of the work by GRC is an integrated sensor orientation system for a range of uses including airborne applications with a digital single lens reflex camera sensor. The system has been operational on a number of flight trials and The University of Nottingham have been investigating the potential of the system for photogrammetric applications.

The paper will introduce the system and operation, and then present the results to-date produced by The University of Nottingham for photogrammetric applications.

## 1. INTRODUCTION

### 1.1 Background

There are now available excellent integrated sensor orientation systems for the direct measurement of sensor position and attitude using GPS and IMU technology. With the maturity of these systems has come a wider interest in using this technology in an ever-increasing range of applications. The photogrammetric and remote sensing community have enthusiastically welcomed this technology as it brings about enhanced solutions and significant increases in efficiency. The use of integrated systems for laser scanning and high quality mapping from imaging scanners has been fundamental to their success. With a variety of applications, there comes a need for a variety of solutions, balancing quality and cost. At both extremes, for example high accuracy engineering applications and lower accuracy environmental geographical studies challenges are presented to the technology. Even at the lower accuracy requirements there is a demand for achieving the solution in a cost effective way.

The Geospatial Research Centre (NZ) Ltd (GRC) has been developing integrated sensor orientation technology and exploring the applications for low cost but effective (fit-for-purpose) solutions. It set the following aims for the system:

- Cost-effective for small area (local) surveys
- Enable high spatial and temporal resolution
- Enable flexibility in hardware in response to accuracy and cost
- Operating efficiently.

This led the GRC to consider a range of imaging sensors including thermal cameras and digital single lens reflex cameras. At the present time there is a rapid pace of development in digital single lens reflex cameras which is providing them with added photogrammetric potential.

With demands from the areas of forestry, infrastructure assessment/pre-surveys, agricultural and environmental monitoring the GRC was keen to focus some of the early activity on local surveys requiring the production of image based products typically georeferenced aerial image mosaics and ortho-images. The products for this type of application require fast, simple and therefore efficient processing procedures, keeping the technical photogrammetric aspects to a minimum. The aim for the accuracy level for the feature and information extraction was in the order of 1-2m.

### 1.2 Aims and objectives

The overall aim of the research undertaken at The University of Nottingham was to investigate the geometric potential of using

---

\* Corresponding author.

the integrated system developed. The aim of this paper is to present results from the initial stage of this research which is investigating the georeferencing of small format imagery.

### 1.3 Methodology

The methodology is based of the following stages:

1. Understanding the integrated system
2. Creation of a test site with available:
  - a. Images;
  - b. ground control and check points;
  - c. DTM.
3. A comparison of aerial triangulation (AT) using varying amounts of ground control.
4. An assessment of ortho-images produced from selected AT results.

The method of analysis is based on image, control and check point residuals.

## 2. TECHNOLOGY

### 2.1 System hardware

The GRC-developed Aerial Mapping Package (AMP) consists of 3 self contained hardware modules as shown in figure 1:

- Sensor Module (digital camera and Inertial Measurement Unit)
- Aerial Mapping Package Core (GNSS receiver, support controls and power electronics, battery, and data logging)
- Flight Management Display System (for directing the pilot via light bar and / or displaying required flight lines)

The Sensor Module is on the left hand side of the image (camera pointing up to be visible) and the AMP Core is to the front.

This cost-effective AMP system was designed for mounting on a light aircraft, helicopter or micro-light where the camera and IMU would be co-located in a package smaller than a shoe box with the GPS, data logging, etc. stored where possible in a similarly sized unit. To date, the AMP system has been successfully installed and flight tested in New Zealand on the following platforms:

- Microlight (Airborne XT)
- Cessna 172
- Piper Archer/Piper Cub

The package is self powered for up to 6 hours with a single on-off switch designed to greatly simplify in-field use.

Although The University of Nottingham team used LPS to process the trial data in this paper, GRC also developed its own in-house direct geo-referencing software offering the flexibility to use a variety of IMU's and GNSS data and designed around the special nature of very small format, low altitude aerial triangulation. In post-processing form, this software is capable of running in an automatic processing mode which is designed for a non-expert user (although the inevitable tuning of input parameters, weights, etc. does lead to output improvements if the user knows what they are doing).



Figure 1. GRC aerial mapping package (Mills et al., 2009)

For the specific, early, trial flight presented in this paper, the following hardware was used:

- Dual frequency GPS (Novatel board)
- iMar IMU
- Canon digital SLR (400 series) with a fixed 28mm lens (nominal)

The GPS and IMU used were of excellent quality in the initial flight trials (completed mid 2008) in order to remove, as much as possible, OEM hardware problems from the integration development program.

The image capture requirements for this specific trial, flown August 2008, were for 15cm resolution imagery that could be directly geo-referenced from on-board GPS/IMU data (plus existing 25m DTM and boresight, lever arm calibration, etc.) to an absolute accuracy on the ground of +/- 1m (1sd) in plan.<sup>1</sup>

### 2.2 System calibration

Before any photogrammetric processing can take place the system needs to be calibrated through a boresight calibration to give the rotation matrix and the lever arm calibration is necessary to take into account the distance of the GPS antenna from the camera.

The lever arm was measured before the flight (a simple process in a microlight as there are no physical barriers to limit direct

<sup>1</sup> Other trials have since generated data with ground resolutions as high as 25mm over urban, rural, forested, flat and mountainous regions across South Island, New Zealand. It is hoped that further assessment / analysis of this data will be completed by The University of Nottingham team in the coming months.

measurement / view). The boresight data was captured at the start of the flight in the normal way over the GRC's calibration site at the home airfield (Rangiora, NZ).

### 3. TRIALS, RESULTS AND ANALYSIS

#### 3.1 Test site

The test site chosen is a rural landscape in New Zealand. The platform was a micro-light aircraft which is not an easy airborne platform to capture traditional images with 60% forward and 20% lateral overlap. So even with the flight management system the imagery was far from being conventional, figure 2 shows the block of images selected for this trial. This makes the direct georeferencing even more challenging as the position and orientation of the images is so variable.

Ground control points (GCPs) were captured in the field using a survey grade (dual-frequency) Trimble GPS receiver and base station and processed in both the GRC GPS processing engine (POINT) and GrafNav.

A 25m DTM was available, originally produced by Landcare Research ([www.landcareresearch.co.nz](http://www.landcareresearch.co.nz)) from existing 1:50,000 map contours.

#### 3.2 Imagery

The images were captured using a Canon Digital SLR camera with a focal length of 28.5010mm, a 5.7  $\mu\text{m}$  pixel size and a sensor size of 3888x2592 pixels. 303 images were selected to form a block resembling that of a traditional aerial survey with 5 strips, see figure 2.

#### 3.3 Aerial triangulation results

##### 3.3.1 Observations and computations

A total number of 22 coordinated ground points in 7 clusters were available and measured on the images and a total of 2500 automatic tie points were extracted.

##### Aerial Triangulation Results – Trial 1

The AT solution is calculated using only the in-flight GPS/IMU information which is kept fixed. All the available control points are set as check points. The Jacobsen's self calibration model is used with 4 additional parameters. The results are shown in table 1 and figure 2.

Total image unit weight RMSE =	Control Point RMSE (no pts)	Check Point RMSE (no pts)
6.6 $\mu\text{m}$		
Ground X m	0.000 (0)	0.601 (21)
Ground Y m	0.000 (0)	0.743 (21)
Ground Z m	0.000 (0)	5.613 (21)
Image x $\mu\text{m}$	0.0 (0)	20.4 (185)
Image y $\mu\text{m}$	0.0 (0)	12.2 (185)

Table 1. AT results from trial 1

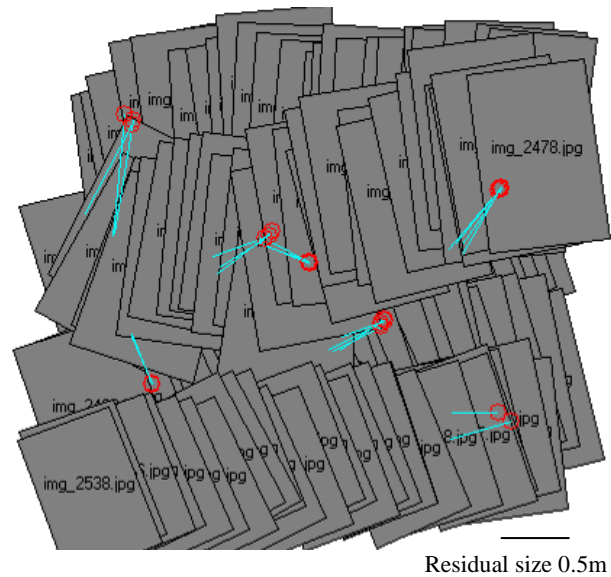


Figure 2. Trial 1 block showing residuals ( $\Delta$  = control points, O = check points)

##### Aerial Triangulation Results – Trial 2

The AT solution is calculated using the in-flight GPS/IMU information as initial values but left to float. Twenty one control points are used with no self-calibration model used. The results are shown in table 2.

Total image unit weight RMSE =	Control Point RMSE (no pts)	Check Point RMSE (no pts)
3.8 $\mu\text{m}$		
Ground X m	0.009 (21)	0.000 (0)
Ground Y m	0.110 (21)	0.000 (0)
Ground Z m	0.336 (21)	0.000 (0)
Image x $\mu\text{m}$	5.9 (185)	0.0 (0)
Image y $\mu\text{m}$	3.7 (185)	0.0 (0)

Table 2. AT results from trial 2

##### Aerial Triangulation Results – Trial 3

The AT solution is calculated using the in-flight GPS/IMU information as initial values but left to float. Twenty one control point are used. The Jacobsen's self calibration model is used with 4 additional parameters, see table 3.

Total image unit weight RMSE =	Control Point RMSE (no pts)	Check Point RMSE (no pts)
3.8 $\mu\text{m}$		
Ground X m	0.098 (21)	0.000 (0)
Ground Y m	0.099 (21)	0.000 (0)
Ground Z m	0.242 (21)	0.000 (0)
Image x $\mu\text{m}$	5.6 (185)	0.0 (0)
Image y $\mu\text{m}$	5.3 (185)	0.0 (0)

Table 3. AT results from trial 3

##### Aerial Triangulation Results – Trial 4

The AT solution is calculated using the in-flight GPS/IMU information as initial values with a standard deviation (std) of

0.20m,0.20m,0.50m for XYZ and 0.01 degrees for the rotation. Twenty one control points are used but no check points. The Jacobsen's self calibration model is used with 4 additional parameters.

Total image unit weight RMSE = 4.7 $\mu$ m	Control Point RMSE (no pts)	Check Point RMSE (no pts)
Ground X m	0.100 (21)	0.000 (0)
Ground Y m	0.123 (21)	0.000 (0)
Ground Z m	0.656 (21)	0.000 (0)
Image x $\mu$ m	8.3 (185)	0.0 (0)
Image y $\mu$ m	6.7 (185)	0.0 (0)

Table 4. AT results from trial 4

### Aerial Triangulation Results – Trial 5

The AT solution is calculated using the in-flight GPS/IMU information as initial values with a std of 0.20m,0.20m,0.50m for XYZ and 0.01 degrees for the rotation angles. 5 control points are used, four in the corners and one in the centre of the block, and the remaining points set as check points. The Jacobsen's self calibration model is used with 4 additional parameters.

Total image unit weight RMSE = 4.5 $\mu$ m	Control Point RMSE (no pts)	Check Point RMSE (no pts)
Ground X m	0.115 (5)	0.140 (16)
Ground Y m	0.120 (5)	0.191 (16)
Ground Z m	1.831 (5)	1.882 (16)
Image x $\mu$ m	14.8 (44)	4.8 (141)
Image y $\mu$ m	13.8 (44)	3.9 (141)

Table 5. AT results from trial 5

### Aerial Triangulation Results – Trial 6

The AT solution is calculated using the in-flight GPS/IMU information as initial values with a std of 0.20m,0.20m,0.50m for XYZ and 0.01 degrees for the rotation angles. 1 control points is used and the remaining points set as check points. The Jacobsen's self calibration model is used with 4 additional parameters.

Total image unit weight RMSE = 4.3 $\mu$ m	Control Point RMSE (no pts)	Check Point RMSE (no pts)
Ground X m	0.006 (1)	0.450 (20)
Ground Y m	0.299 (1)	0.650 (20)
Ground Z m	3.871 (1)	4.636 (20)
Image x $\mu$ m	15.9 (12)	5.0 (173)
Image y $\mu$ m	23.7 (12)	4.0 (173)

Table 6. AT results from trial 6

### Aerial Triangulation Results – Trial 7

The AT solution is calculated using the in-flight GPS/IMU information as initial values but left to float. 5 control points in the corners of the block were used and 16 check points. The Jacobsen's self calibration model is used with 4 additional parameters.

Total image unit weight RMSE = 3.7 $\mu$ m	Control Point RMSE (no pts)	Check Point RMSE (no pts)
Ground X m	0.030 (5)	0.172 (16)
Ground Y m	0.103 (5)	0.120 (16)
Ground Z m	0.388 (5)	0.449 (16)
Image x $\mu$ m	3.9 (43)	4.7 (142)
Image y $\mu$ m	3.5 (43)	3.7 (142)

Table 7. AT results from trial 7

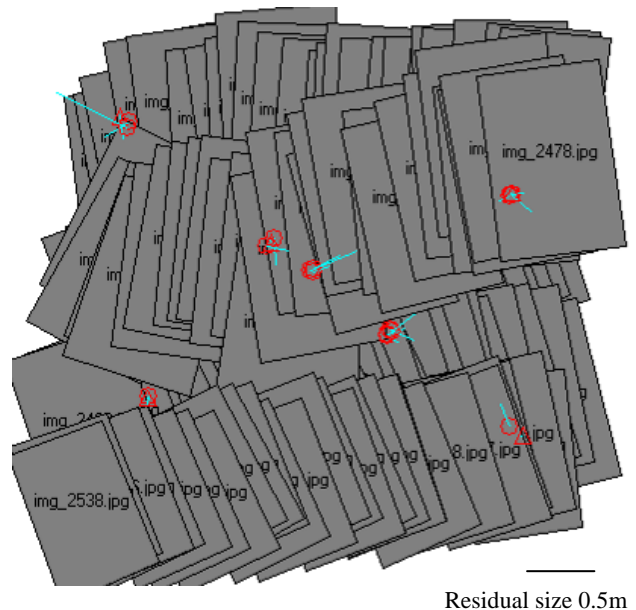


Figure 3. Trial 7 block showing residuals ( $\Delta$  = control points, O = check points)

Table 8 shows a summary of the variations in the solutions.

Trial No	In-flight control	Self-calibration	No of ground control points	No of check points
1	√	√	0	21
2			21	0
3		√	21	0
4	√	√	21	0
5	√	√	5	16
6	√	√	1	20
7		√	5	16

Table 8. Summary of variations in AT solutions

### 3.3.2 Aerial Triangulation - analysis of results

The automatic measurement of the tie points in the aerial triangulation proved to be challenging with the small format images and the slightly irregular flight lines. Early trials, even with blunder detection operating proved difficult to achieve a solution. After manual editing of tie-point outliers a solution was obtained producing a good fit to the ground control. A number of trials were undertaken with various control and self-calibration scenarios. Good solutions were obtained when sufficient ground control is used (tables 2, 3, 4). As the in-flight

control is introduced and becomes more influential the quality drops off (tables 4, 5, 1). Figure 2 also shows some systematic pattern to the residuals on the check points with no ground control. Tables 2 and 3, show that the use of a self-calibration model helps. Of particular interest is table 1 which is using only the in-flight control which shows that for applications requiring plan positioning, where heighting is not so critical, the in-flight control is providing good results. This is relative to the applications (specifications) that the system was designed to support.

With these applications in mind ortho-images were produced using the available 25m DTM with only a small amount of ground control, 5 points (trial 7) and no ground control (trial 1).

### 3.3.3 Ortho-image Generation

An ortho-image produced with the best aerial triangulation results (trial 7) is shown in figure 4. Images edges have been left to show where the joins are.



Figure 4. Ortho-image from good AT results (AT trial 7)

A representative fit across cut lines is illustrated in figure 5.

A quantitative assessment was performed on the ortho-image in figure 4 by measuring the plan position of the ground control points. 10 control points were measured and their planimetric residuals are shown in table 9.



Figure 5. Typical examples of the ortho-image cut lines (AT trial 7)

Control Pt ID	Residual (absolute magnitude, m)
25	0.23
26	0.72
10	0.24
11	0.17
16	1.30
39	0.77
14	0.34
15	0.42
35	1.27
36	0.87
Mean	0.63

Table 9. Planimetric quality assessment of the ortho-image created from AT trial 7

Figure 6 shows the ortho-image generated using the results from the in-flight control only solution (trial 1).

A quantitative assessment was performed on the ortho-image in figure 6 by measuring the plan position of the ground control points. 10 control points were measured and their planimetric residuals are shown in table 10.



Figure 6. Ortho-image generated from using only in-flight control in the AT (AT Trial 1)

A representative fit across cut lines is illustrated in figure 7.



Figure 7. Typical examples of the ortho-image cut lines (AT trial 1)

From the visual inspection of the ortho-images the use of ground control has improved the results by the order of 50%. However, with no ground control the mean magnitude of the residuals at 10 of the control points are still only just over a 1m and very useful for some applications

Control Pt ID	Residual (absolute magnitude, m)
25	2.10
26	1.89
10	0.31
11	0.92
16	2.03
39	0.32
14	0.49
15	0.26
35	2.02
36	1.91
Mean	1.23

Table 10. Planimetric quality assessment of the ortho-image created from AT trial 1

#### 4. CONCLUSIONS AND FUTURE ACTIVITIES

It is clear that the original design brief (for generating cost effective, fast turnaround, high resolution images geo-referenced to at least 1m absolute accuracy in plan) has been met by the use of only in-flight control presented in this paper. However, it is also worth noting that, as always, the addition of even one good ground control point can make a big difference in the aerial triangulation and subsequent orthophoto generation processes.

Whilst the comparison between figure 5 and 7 clearly demonstrates the benefits of including minimal ground control in the integrated solution, it is suggested that the less than perfect output in figure 7 is actually all that is required in many applications (e.g. primary forestry production or damage assessments).

It is interesting to note the larger than expected height errors observed, further discussions with the New Zealand based team are ongoing to determine exactly what might have caused this.

Further investigation is also suggested by this paper across a range of other aspects highlighted by this short study including:

- The use of long range, kinematic PPP processing to generate in-flight GPS coordinates;
- The analysis of the distributions of residuals from the aerial triangulation results (as only the summaries have been presented here).

#### 5. REFERENCES

##### References from Other Literature:

Mills, S., Park, D., Hide., C., Barnsdale, K., Pinchin, J., 2009. Integrated GNSS, IMU, and imagery for automatic orthomosaics generation. In: *The Institute of Navigation (ION) proceedings*.

##### 5.1 Acknowledgements

The authors would like to thank Geospatial Research Centre (NZ) Ltd for access to the data and additional discussions and Lincoln University's Bio-protection Centre of Research Excellence (for ground access to the test site).